Restart Strategy for Sensorless PMSM Drive with Single Zero Voltage Vector in Railway Application

Fei Du. Student member[1], Jian Li. Senior member[2], and GuoFeng Li. Senior member[1]
[1] Dalian University of Technology, China
[2] Huazhong University of Science and Technology, China

***Abstract*-- This paper proposes a control algorithm and a restart method for permanent magnet synchronous motors without position sensors in railway application. The method combines a Luenberger observer and a sensorless observation method based on PLL, allowing for accurate observation of rotor position and speed within the high-speed range of the motor. Additionally, the method utilizes the setting of the contactor to estimate the initial position and speed during the restart process using the current generated by a single zero voltage vector, enabling precise estimation of the motor's speed and position in the flux-weakening region. The effectiveness of the proposed algorithm is demonstrated through simulation.**

***Index Terms*-- rotor position estimation scheme, Luenberger observer, PLL, restart strategy, single zero voltage vector**

I. INTRODUCTION

In high-power Permanent Magnet Synchronous Motors (PMSM) applications, particularly in the region of railway application, the detection of position sensors is susceptible to inaccuracies caused by non-ideal environmental conditions. Hence, the sensorless control has garnered significant interest. The precision of rotor position measurement directly impacts the operational performance of the motors. By utilizing the back electromotive force (EMF) estimation technique, the sensorless control of PMSM in the medium and high speed regions can be enhanced in terms of reliability and accuracy [1]. This method can be implemented in both the rotating coordinate system and the stationary coordinate system.

Traditional methods for position estimation without the use of dedicated position sensors include sliding mode observer (SMO), motor reference adaptive systems (MRAS), observer based on Kalman filters and Luenberger observer [2-5]. When a motor undergoes a restart, there is a critical need for the observer to achieve rapid stabilization, which places higher demands on its dynamic performance. Traditional sliding mode observer often incorporate filtering components, which can lead to a decrease in their dynamic performance. Positionless sensor algorithms based on MRAS heavily rely on the steady-state model of the motor, resulting in reduced accuracy in estimating position and speed during dynamic motor processes. The Kalman filter algorithm, although capable of achieving high accuracy, requires multiple iterations to converge and suffers from a significant computational burden. As a result, its application is limited in practical scenarios.

For position estimation, there are several methods commonly used, including direct calculation, PLL (PLL), and Luenberger observer [6-8]. The direct calculation method exhibits high sensitivity to noise and lacks stability. Luenberger observer, while providing accurate position estimation, involve complex modeling and require knowledge of the motor's moment of inertia. Traditional PLLs in position estimation employ a PI controller, which offers a relatively straightforward design. However, the stability and speed correlation of traditional PLLs heavily rely on fixed PI parameters. The challenge arises during motor restarts, as the motor speed is unknown, leading to uncertain stability of the PLL.

The conventional technique employed for motor restarting utilizes single or multiple zero voltage vectors [9-10]. The motor's speed and position are determined based on the short-circuit current generated by the zero voltage vectors. However, this technique assumes that the sampled current is solely produced by the zero voltage vector, which is not the case in the flux-weakening region. In this region, the sampled current may contain uncontrolled rectification current due to the EMF exceeding the DC voltage. The traditional approach of using multiple zero voltage vectors fails to eliminate the current deviation caused by uncontrolled rectification, leading to significant calculation errors. Additionally, determining the time interval between the multiple zero voltage vectors can be challenging. In railway applications, contactors are employed between the inverter and PMSM [11]. By setting the contactor during a single zero voltage vector process, uncontrolled rectification can be mitigated. However, the conventional method for estimating single zero voltage vector's accuracy is not high, which may result in overcurrent in the flux-weakening region.

To address the aforementioned issues, this paper proposes two methods: Luenberger observer combined with PLL and contactor combined with single zero voltage vector method. The Luenberger observer can calculate the EMF of the motor through the measurement of motor current, and the PLL can calculate the position and speed of the PMSM. The contactor combined with single zero voltage vector method can eliminate the effect of uncontrolled rectification in the sampled current, reduce the speed and position estimation error, and achieve fast

restart in flux-weakening region. When the PMSM enters the flux-weakening region, the contactor will cut off the inverter supply, and then restart the motor through the single zero voltage vector method. This can improve the restart probability and avoid the instability of the motor in flux-weakening region.

II. Sensorless PMSM Drive System

In order to achieve sensorless control and restart in the flux-weakening region of a PMSM, it is essential to have an accurate motor model and a reliable restart method. The observer model will be derived in this section. The restart method will be described in the next section.

A. PMSM Modeling

Assuming a symmetric three-phase stator winding and neglecting stator and rotor magnetic saturation, eddy current losses, hysteresis losses, iron losses, and copper losses, while considering constant motor parameters during the temperature rise process, the basic voltage equation for a PMSM in a rotating coordinate system can be expressed as follows.

$$\begin{bmatrix} u_d \\ u_q \end{bmatrix} = \begin{bmatrix} R_s + pL_d & -\omega_e L_q \\ \omega_e L_d & R_s + pL_q \end{bmatrix} \begin{bmatrix} i_d \\ i_q \end{bmatrix} + \begin{bmatrix} 0 \\ \psi_f \omega_e \end{bmatrix} \quad (1)$$

Equation (1) provides the actual rotor position information. However, it is worth noting that the diagonal elements of the impedance matrix in (1) are asymmetric, which poses challenges for observer design. To address this issue, the equation can be transformed symmetrically, leading to the following equation.

$$\begin{bmatrix} u_d \\ u_q \end{bmatrix} = \begin{bmatrix} R_s + pL_d & -\omega_e L_q \\ \omega_e L_q & R_s + pL_d \end{bmatrix} \begin{bmatrix} i_d \\ i_q \end{bmatrix} + \begin{bmatrix} 0 \\ E \end{bmatrix} \quad (2)$$

where E represents the extended back EMF(EEMF), and the equation is

$$E = (L_d - L_q)(\omega_e i_d - p i_q) + \psi_f \omega_e \quad (3)$$

Compared to the PMSM equation based on the d-q axis, the motor equation formulated using the α-β axis offer a more convenient way to describe the relationship between EEMF and the rotor position θ. By symmetrical rewriting of the inductances, (1) can be derived.

$$\begin{bmatrix} u_\alpha \\ u_\beta \end{bmatrix} = \begin{bmatrix} R_s + pL_d & \omega_e (L_d - L_q) \\ -\omega_e (L_d - L_q) & R_s + pL_d \end{bmatrix} \begin{bmatrix} i_\alpha \\ i_\beta \end{bmatrix} + \begin{bmatrix} E_\alpha \\ E_\beta \end{bmatrix} \quad (4)$$

where E_α and E_β represent the components of the EEMF in the stationary coordinate system, and the equation is

$$\begin{bmatrix} E_\alpha \\ E_\beta \end{bmatrix} = \left[(L_d - L_q)(\omega_e i_d - p i_q) + \psi_f \omega_e \right] \begin{bmatrix} -\sin\theta \\ \cos\theta \end{bmatrix} \quad (5)$$

Equation (2) and (4) can both be utilized as models for the observer in a sensorless system, where the observed variable is the expanded counter electromotive force or its components. The observer design presented in this paper adopts the voltage equation in the stationary coordinate system.

By expressing (4) and (5) in the form of state equation, we can derive the basic voltage (6) for the observer.

$$\begin{cases} \dfrac{di_\alpha}{dt} = -\dfrac{R_s}{L_d} i_\alpha - \dfrac{\omega_e (L_d - L_q)}{L_d} i_\beta + \dfrac{u_\alpha}{L_d} - \dfrac{E_\alpha}{L_d} \\ \dfrac{di_\beta}{dt} = -\dfrac{R_s}{L_d} i_\beta + \dfrac{\omega_e (L_d - L_q)}{L_d} i_\alpha + \dfrac{u_\beta}{L_d} - \dfrac{E_\beta}{L_d} \end{cases} \quad (6)$$

From (5), the following relationship can be obtained

$$\begin{bmatrix} \dot{E}_\alpha \\ \dot{E}_\beta \end{bmatrix} = \begin{bmatrix} -\omega_e E_\beta \\ \omega_e E_\alpha \end{bmatrix} \quad (7)$$

By combining (4) and (7), the full-order model of a PMSM is obtained, which can be utilized for observer design.

$$\frac{d}{dt}\boldsymbol{X} = \begin{bmatrix} \boldsymbol{a}_{11} & \boldsymbol{a}_{12} \\ 0 & \boldsymbol{a}_{22} \end{bmatrix} \boldsymbol{X} + \begin{bmatrix} \boldsymbol{b} \\ 0 \end{bmatrix} \boldsymbol{u} \quad (8)$$

where

$$\boldsymbol{X} = [\, i_\alpha \;\; i_\beta \;\; E_\alpha \;\; E_\beta \,]^T \quad ,$$

$$\boldsymbol{a}_{11} = \frac{1}{L_d} \begin{bmatrix} -R_s & -\omega_e (L_d - L_q) \\ \omega_e (L_d - L_q) & -R_s \end{bmatrix} \quad ,$$

$$\boldsymbol{a}_{22} = \omega_e \begin{bmatrix} 0 & -1 \\ 1 & 0 \end{bmatrix} \;,\; \boldsymbol{a}_{22} = \omega_e \begin{bmatrix} 0 & -1 \\ 1 & 0 \end{bmatrix} \;,\; \boldsymbol{k} = \frac{1}{L_d} \begin{bmatrix} k & 0 \\ 0 & k \end{bmatrix} \;,$$

$$\boldsymbol{m} = \frac{1}{L_d} \begin{bmatrix} m & 0 \\ 0 & m \end{bmatrix}$$

B. Observer model

According to (8), a Luenberger observer can be designed in the stationary coordinate system. The observer model is given as follows:

$$\frac{d}{dt}\hat{\boldsymbol{X}} = \begin{bmatrix} \boldsymbol{a}_{11} & \boldsymbol{a}_{12} \\ 0 & \boldsymbol{a}_{22} \end{bmatrix} \hat{\boldsymbol{X}} + \begin{bmatrix} \boldsymbol{b}_1 \\ \boldsymbol{b}_2 \end{bmatrix} \boldsymbol{u} + \begin{bmatrix} \boldsymbol{k} \\ \boldsymbol{m} \end{bmatrix} \tilde{\boldsymbol{i}} \quad (9)$$

where, $\tilde{\boldsymbol{i}} = \begin{bmatrix} i_\alpha - \hat{i}_\alpha \\ i_\beta - \hat{i}_\beta \end{bmatrix}$

where the symbol '^' represents an estimated value, and the symbol '~' indicates the difference between estimated and actual values. Here, k and m denote observer gains that are determined through stability analysis.

C. Observer stability analysis

The stability of the Luenberger observer relies on the selection of suitable values for k and m. Designing appropriate values for k and m is crucial as it ensures the system's stability and enables fast convergence. The error matrix of the system can be derived from (8) and (9), resulting in (10).

$$A - KC = \begin{bmatrix} \dfrac{-R_s + \mathrm{j}\omega_e (L_d - L_q)}{L_d} - k_1 & -\dfrac{1}{L_d} \\ -k_2 & \mathrm{j}\omega_e \end{bmatrix} \quad (10)$$

The corresponding characteristic equation is shown in

(11).

$$f(\lambda)=\lambda^2+\frac{R_s-\mathrm{j}\omega_e(L_d-L_q)+k_1L_d-\mathrm{j}\omega_eL_d}{L_d}\lambda+\frac{\mathrm{j}\omega_eR_s+\omega_e(L_d-L_q)+k_1\mathrm{j}\omega_eL_d-k_2}{L_d} \tag{11}$$

According to the Lyapunov's first method, in order to make the observer tend to be stable, that is, the error tends to 0, then for the equation, all roots should have negative real parts. Based on this stability theory, the value of neutralization in the feedback gain matrix matrix can be determined, which is no longer described in detail in this paper.

D. PLL based position observer

The EEMF observed through (9) can be directly utilized for calculating the rotor position information, and integration of the EEMF can provide the motor speed information. However, this approach introduces noise and factors such as parameter deviations, resulting in significant fluctuations in the estimated rotor position. To address these issues, a PLL structure can be employed, which effectively suppresses the influence of noise and parameter deviations.

The fundamental structure of a conventional PLL comprises a PI controller, where the input is the angular error and the output is the motor angular velocity. When the estimation errors of the angle and the EEMF are small, (12) can be obtained.

$$\begin{aligned}\varepsilon&=E\left(\theta_e-\hat{\theta}_e\right)\approx E\sin\left(\theta_e-\hat{\theta}_e\right)\\&=E\sin\theta_e\cos\hat{\theta}_e-E\sin\hat{\theta}_e\cos\theta_e\\&\approx-\hat{E}_\alpha\cos\hat{\theta}_e-\hat{E}_\beta\sin\hat{\theta}_e\end{aligned} \tag{12}$$

The design of the PLL can be performed based on (12). However, it is evident from (12) that when the PI parameters in the PLL are fixed, an increase in speed results in an increase in the EEMF. This, in turn, leads to changes in the closed-loop characteristic roots of the system, causing variations in the system bandwidth, which can be detrimental to the stability of the observer. To address this issue, a normalized PLL structure is adopted, as depicted in Fig. 1. This structure helps mitigate the variations in the closed-loop characteristic roots with changes in speed, thereby ensuring a stable and robust observer.

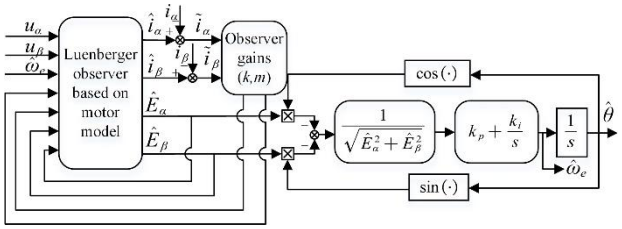

Fig. 1. Scheme of position estimation based Luenberger observer

The per-unit PLL is designed by (13).

$$\begin{cases}\hat{E}_{\alpha\_pu}=\dfrac{\hat{E}_\alpha}{\sqrt{\hat{E}_\alpha^2+\hat{E}_\beta^2}}\\[2ex]\hat{E}_{\beta\_pu}=\dfrac{\hat{E}_\beta}{\sqrt{\hat{E}_\alpha^2+\hat{E}_\beta^2}}\end{cases} \tag{13}$$

By normalizing the PLL using (13), the amplitude of the EEMF can be brought close to 1. This normalization process helps preserve the maximum amount of information from the EEMF, enabling accurate estimation of the motor rotor position. Following the normalization of the PLL, the closed-loop transfer function can be represented by (14).

$$G_{\mathrm{PLL\_Pu}}=\frac{k_ps+k_i}{s^2+k_ps+k_i} \tag{14}$$

The parameters of the PLL can be designed using pole placement technique, which enables the selection of suitable parameters for position observation at different speeds. This approach achieves decoupling between the PLL bandwidth and the speed, ensuring optimal performance of the observer.

III. Restart Method in the Flux-weakening Region

In a position control system without position control, the observer may encounter difficulties during the restart moment due to the absence of accurate voltage information. Therefore, the rotor position and speed information of the motor are missing at the restarting time. However, it is necessary to estimate the rotor position and speed at the restarting time, and it is also an important information that can achieve successful restarting under small current shocks. In this paper, the rotor position and speed are calculated by using the short-circuit current generated by a single zero-voltage pulse at the time of restarting. At the same time, in order to ensure that the belt speed restarting can be successfully completed in the weak magnetic region, the opening and closing of the contactor is used to avoid the influence of uncontrolled rectification on the sampling current, which ensures the accuracy of rotor position information and speed estimation.

To address these requirements, this paper presents a system configuration, depicted in Fig. 2.

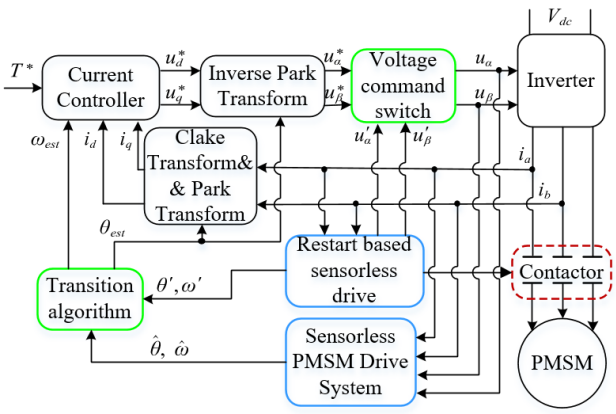

Fig. 2. The system configuration proposed in this paper

A. *Restart system settings*

In the process of realizing the restart, uncontrolled rectification that occurs in the flux-weakening region can impact speed calculations and result in deviations. To reduce its impact, this paper proposes a new restart method shown by the restart unit in Fig.2. The execution flow chart of this restart unit is given in Fig. 3. In the proposed method, the contactor between the inverter and the motor is used to achieve the following objectives:

a) Protects the motor from disconnection between the inverter and the motor at the moment of failure;

b) By ensuring that the current remains at zero, it is possible to eliminate the impact of uncontrolled rectification during the restarting process.

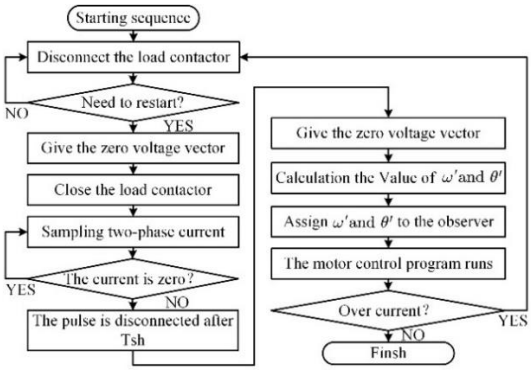

Fig. 3. Flowchart of proposed restart method

Fig. 4 shows the timing diagram of various signals and related state variables in the process of restart. The method is placed in the timer interrupt, which can realize higher frequency current sampling, and can control the zero voltage pulse action time more accurately.

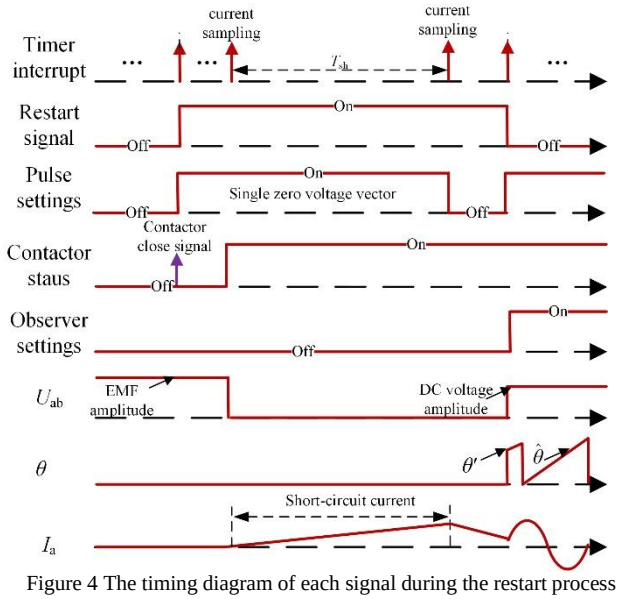

Figure 4 The timing diagram of each signal during the restart process

Fig. 5 shows the short circuit current vector(I_s) when using zero voltage vector. The initial rotor position (θ_0) is the angle between I_s and the α-axis, the value of θ_0 can be determined from the sampled current. In a rotating coordinate system, the angle between Is and the d-axis can be expressed as θ_1, and the value of θ_1 can be determined by (19). θ' is the angle between the α-axis and the d-axis.

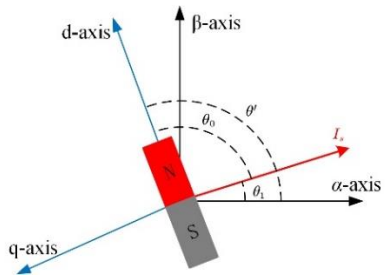

Fig. 5. Short-circuit current vectors by using zero vectors

B. *Position and speed calculation at restart time*

The restart method utilizes the voltage equation of the PMSM in the rotating coordinate system. By employing the zero-voltage vector, a short-circuit current is generated, allowing for the estimation of the motor speed and position in a short period of time. Assuming that the sampling time is sufficiently short, the stator resistance (R_s) can be considered negligible. The voltage equation with the zero-voltage vector can be represented by (15).

$$\begin{bmatrix} 0 \\ 0 \end{bmatrix} = \begin{bmatrix} pL_d & -\omega' L_q \\ \omega' L_d & pL_q \end{bmatrix} \begin{bmatrix} i_d \\ i_q \end{bmatrix} + \begin{bmatrix} 0 \\ \psi_f \omega' \end{bmatrix} \tag{15}$$

Among them, the symbol ‘’ represents the estimated value in the process of recast with speed.

If the initial value of the current is 0, the short-circuit current (16) can be obtained by Laplace transform. In addition, $\sin(\omega_e T_{sh})$ and $\cos(\omega_e T_{sh})$ can be regarded ($\omega_e T_{sh}$) and ($1-\omega_e T_{sh}/2$).

$$[i_s(T_{sh})] = \begin{bmatrix} i_d(T_{sh}) \\ i_q(T_{sh}) \end{bmatrix} \cong \begin{bmatrix} -\dfrac{\psi_f (\omega' T_{sh})^2}{2L_d} \\ -\dfrac{\psi_f \omega' T_{sh}}{L_q} \end{bmatrix} \tag{16}$$

When a short-circuit current vector is introduced, θ_1 can be obtained by sampling I_a, I_b and performing coordinate transformation. The estimated rotor initial position θ_0 is expressed as in (17).

$$\theta_0 \cong \tan^{-1}\left(\frac{i_q}{i_d}\right) = \tan^{-1}\left(\frac{L_d \sin(\omega' T_{sh})}{L_q[1-\cos(\omega' T_{sh})]}\right) \tag{17}$$

The angle θ_1 between the current vector and the α-axis can be calculated from i'_α, i'_β obtained by the coordinate transformation of the sampled three-phase current.

$$\theta_1 = \tan^{-1}\left(\frac{i'_\beta}{i'_\alpha}\right) \tag{18}$$

From (16) and (17), it is evident that the calculation of the rotor position relies on the angular velocity of the motor. By expanding (16) using the Taylor series and neglecting higher-order terms, (19) can be derived as an approximation.

$$i_s' = \begin{bmatrix} i_d' \\ i_q' \end{bmatrix} = \begin{bmatrix} -\dfrac{\psi_f}{2L_d}(\omega_e' T_{sh})^2 \\ -\dfrac{\psi_f}{L_q}\omega_e' T_{sh} \end{bmatrix} \tag{19}$$

Available from formula (19)

$$i_s' = \psi_f \sqrt{\frac{(\omega_e' T_{sh})^4}{4L_d^2} + \frac{(\omega_e' T_{sh})^2}{L_q^2}} \tag{20}$$

The traditional single voltage vector injection method often ignores the d-axis current to obtain (21), due to small saliency ratio and low speed. However, the motor used in this paper has a large saliency ratio and runs at high speed. The results calculated by (21) will have a large deviation, and it is easy to cause overcurrent during the restart process. Therefore, it is necessary to optimize the calculation of angular velocity to obtain a more accurate calculation method. Simplify (20) to (22).

$$\omega_e' \approx \frac{L_q i_s'}{\psi_f T_{sh}} \tag{21}$$

$$(\omega_e' T_{sh})^4 + \left(\frac{2L_d \omega_e' T_{sh}}{L_q}\right)^2 - \left(\frac{2L_d i_s'}{\psi_f}\right)^2 = 0 \tag{22}$$

The exact calculation formula of ω' is obtained by solving the equation

$$\omega' = \frac{\sqrt{\sqrt{4k^4 + a^2} - 2k^2}}{T_{sh}} \tag{23}$$

where $k = \dfrac{L_d}{L_q}, a = \dfrac{2 i_s L_d}{\psi_f}$.

Compared with ignoring the influence of d-axis current in [9], the method used in this paper is more accurate in estimating ω'. By using position and speed information obtained from (17), (18) and (23), the rotor angle in the stationary reference frame is

$$\theta' = \theta_1 - \theta_0 \tag{24}$$

IV. Simulation Result

To validate the performance of the proposed observer and the effectiveness of the restart algorithm, the system depicted in Fig. 2 has been implemented in the Matlab/Simulink programming environment. The system's parameters, as outlined in Table I, are utilized for the implementation and evaluation of the proposed methods.

TABLE I
PARAMETERS OF THE PMSM

Parameter	Value	Parameter	Value
Rated DC link voltage (V)	1500	Stator resistance (Ω)	0.0475
Rated speed (rpm)	1900	Amplitude of flux induced by PM (Wb)	0.7654
d-axis inductance (mH)	1.92	q-axis inductance (mH)	4.59
Number of poles	4	Rated torque (Nm)	1257

Fig. 6 and Fig. 7 show the simulation results of motor acceleration and sudden heavy load. In the simulation, the motor speed is accelerated in a ramp mode, and the load mode is constant torque load.

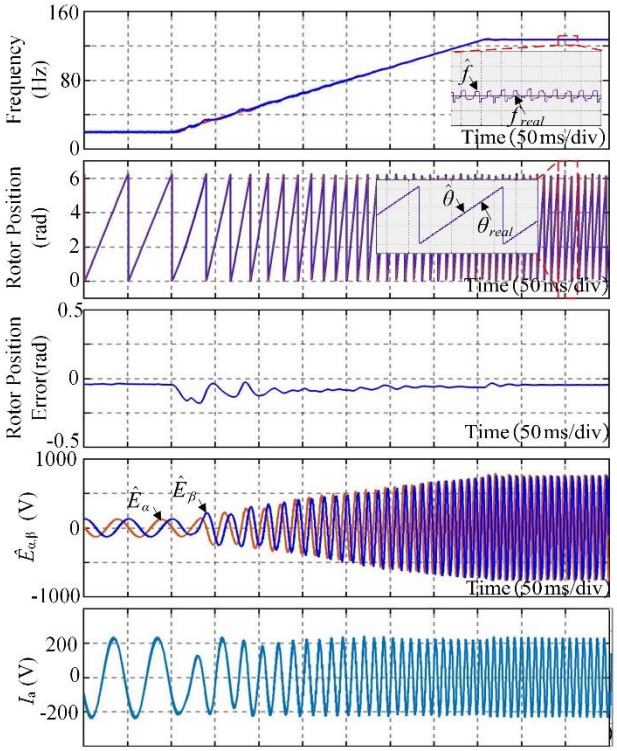

Fig. 6. Speed response of electric pump

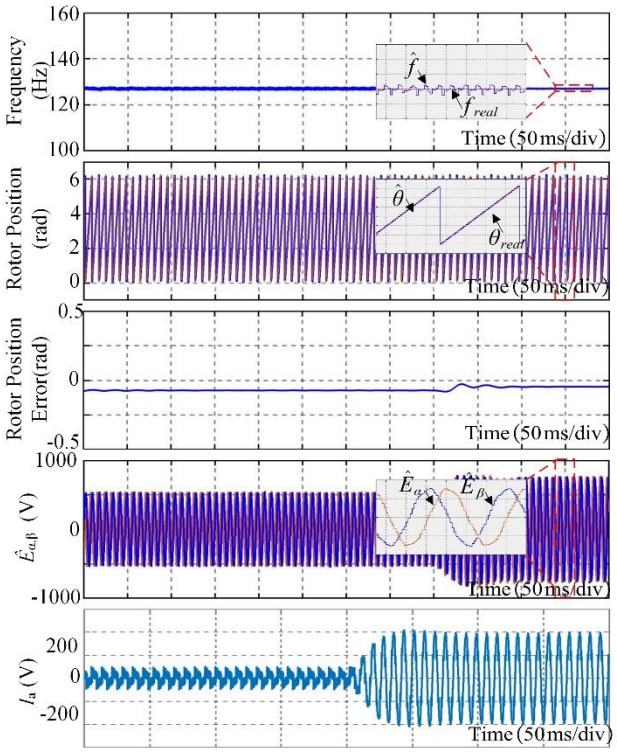

Fig. 7. Torque response of electric pump

Fig. 6 gives the simulation waveform of the motor acceleration, and Fig. 6 gives the simulation waveform of the sudden increase of the motor load. From Fig. 6, it can

be seen that the estimation accuracy of the rotor position and speed is very high whether the motor is accelerated with load or in steady-state operation. The maximum error of the electrical frequency is 0.7 Hz and the electrical angle error is 0.05 rad in steady-state operation. During the acceleration process, the maximum error of the electrical frequency is 2.5 Hz, and the maximum error of the electrical angle is 0.18 rad. The stability of the observer is not related to the speed of the motor, but the error of the observer is large when the speed of the motor is small.

It can be seen from Fig. 7 that the estimation accuracy of rotor position and speed is very high before the observer is loaded before and after loading. Before loading, the estimation error of speed is 1.1 Hz, and the estimation error of rotor position is 0.08 rad. After loading, the estimation error of speed is 0.7 Hz, and the estimation error of rotor position is 0.05 rad.

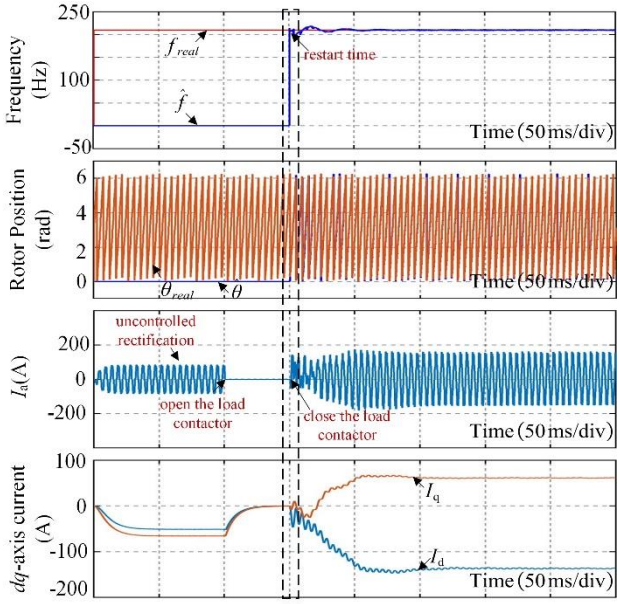

Fig. 8. Simulation results of the restart method of PMSM in flux-weakening region

Fig.8 and Fig.9 shows the experimental simulation results of the motor restarting in the flux-weakening region. The simulation process includes three stages, before disconnecting the contactor, disconnecting the contactor and closing the contactor. In the three stages, the motor runs at a fixed 210Hz electrical frequency. Among them, the content shown in Fig.9 is the content in the wireframe of Fig.8.

From the simulation results, it can be seen that before disconnecting the contactor, because the amplitude of the back EMF is greater than the amplitude of the DC terminal voltage, uncontrolled rectification occurs. After disconnecting the contactor, uncontrolled rectification disappears, and restarting at this time can avoid the impact of uncontrolled rectification. The newly proposed restart algorithm has an error of 4.2 Hz in the electrical frequency calculated at the restart time, and the calculated electrical angle has an error of 0.14 rad. The motor enters a stable working area after 80ms. There was no large current shock during the restart process.

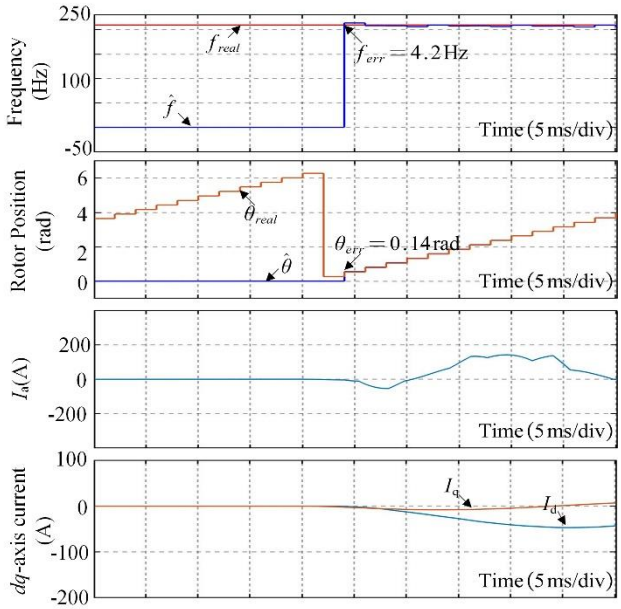

Fig. 9. The content in the wireframe of Fig.8.

V. Conclusions

This paper introduces a position sensorless control system composed of zero voltage vector and Luenberger observer, including flux-weakening position sensorless control and full speed range restart method. In order to estimate the speed and position of PMSM more accurately and quickly, a sensorless observer combining Luenberger observer and PLL is adopted. The single zero voltage vector method is combined with the contactors setting, so as to avoid the influence of uncontrolled rectification in flux-weakening region and realize the restart in the full speed range, and the zero voltage vector method is optimized to make it more accurate. Combined with the position-free control algorithm, the fast and accurate restart of the motor is realized.

References

[1] S. Sul, Y. Kwon and Y. Lee, "Sensorless control of IPMSM for last 10 years and next 5 years," *CES Transactions on Electrical Machines and Systems*, vol. 1, no.2, pp. 91-99, 2017.

[2] C. Gong, Y. Hu, J. Gao, Y. Wang and L. Yan, "An Improved Delay-Suppressed Sliding-Mode Observer for Sensorless Vector-Controlled PMSM," *IEEE Transactions on Industrial Electronics*, vol. 67, no. 7, pp. 5913-5923, July 2020.

[3] X. Sun, Y. Zhang, X. Tian, J. Cao and J. Zhu, "Speed Sensorless Control for IPMSMs Using a Modified MRAS with Gray Wolf Optimization Algorithm," *IEEE Transactions on Transportation Electrification*, vol. 8, no. 1, pp. 1326-1337, March 2022.

[4] P. Niedermayr, L. Alberti, S. Bolognani and R. Abl, "Implementation and Experimental Validation of Ultrahigh-Speed PMSM Sensorless Control by Means of Extended Kalman Filter," *IEEE Journal of Emerging and Selected Topics in Power Electronics*, vol. 10, no. 3, pp. 3337-3344, June 2022.

[5] D. Liang, J. Li, R. Qu and W. Kong, "Adaptive Second-Order Sliding-Mode Observer for PMSM Sensorless

Control Considering VSI Nonlinearity," *IEEE Transactions on Power Electronics*, vol. 33, no. 10, pp. 8994-9004, Oct. 2018.

[6] J. X. Shen, Z. Q. Zhu and D. Howe, "Improved speed estimation in sensorless PM brushless AC drives," *IEEE Transactions on Industry Applications*, vol. 38, no. 4, pp. 1072-1080, July-Aug. 2002.

[7] Z. Novak and M. Novak, "Adaptive PLL-Based Sensorless Control for Improved Dynamics of High-Speed PMSM," *IEEE Transactions on Power Electronics*, vol. 37, no. 9, pp. 10154-10165, Sept. 2022.

[8] Y. Lee and S. -K. Sul, "Model-Based Sensorless Control of an IPMSM With Enhanced Robustness Against Load Disturbances Based on Position and Speed Estimator Using a Speed Error," *IEEE Transactions on Industry Applications*, vol. 54, no. 2, pp. 1448-1459, March-April 2018.

[9] S. Taniguchi, S. Mochiduki, T. Yamakawa, S. Wakao, K. Kondo and T. Yoneyama, "Starting Procedure of Rotational Sensorless PMSM in the Rotating Condition," *IEEE Transactions on Industry Applications*, vol. 45, no. 1, pp. 194-202, Jan.-feb. 2009.

[10] D. -W. Seo, Y. Bak and K. -B. Lee, "An Improved Rotating Restart Method for a Sensorless Permanent Magnet Synchronous Motor Drive System Using Repetitive Zero Voltage Vectors," *IEEE Transactions on Industrial Electronics*, vol. 67, no. 5, pp. 3496-3504, May 2020.

[11] K. Lee S. Ahmed and S. M. Lukic "Universal restart strategy for high-inertia scalar-controlled pmsm drives" *IEEE Trans. Ind. Appl*. vol. 52 no. 5 pp. 4001-4009 Sep. 2016.